



Manchester Metropolitan University

King, Laurie A and Hubert, McKenzie A and Capuano, Christopher and Manco, Judith and Danilovic, Nemanja and Valle, Eduardo and Hellstern, Thomas R and Ayers, Katherine and Jaramillo, Thomas F (2019) A non-precious metal hydrogen catalyst in a commercial polymer electrolyte membrane electrolyser. *Nature nanotechnology*. ISSN 1748-3387

Downloaded from: <http://e-space.mmu.ac.uk/624258/>

Publisher: natureresearch

DOI: <https://doi.org/10.1038/s41565-019-0550-7>

Please cite the published version

<https://e-space.mmu.ac.uk>

29 **Main Text:**

30 The modern-day commercialisation of large-scale polymer electrolyte membrane (PEM)
31 water electrolyzers represents the culmination of decades of fundamental scientific
32 studies involving catalysts, membranes, electrode architectures, and membrane
33 electrode assemblies (MEAs) among other key advancements. Commercial PEM
34 electrolyzers utilize expensive platinum group catalysts such as platinum and iridium,
35 despite their high costs and scarcity, to achieve and maintain high activity over 50,000 h.
36 Terawatt-scale deployment of electrolyzers envisioned for grid resilience require
37 significant reduction of platinum group catalysts and/or replacement by alternative non-
38 platinum group (NPG) catalysts within the device (1). This goal presents many
39 challenges, including the need to tailor catalyst inks, tune deposition methods, and
40 provide stable activity at elevated temperatures, pressures, and current densities, all
41 while demonstrating high activity and durability over the lifetime expected of a
42 commercial system. In this study, we bridge the gap between decades of lab-scale,
43 solution-based, NPG catalyst development and industrial-scale electrolyser operation.
44 We report the first integration of a highly active NPG catalyst (cobalt phosphide, CoP) into
45 a commercial grade PEM electrolyser with >1700 hours of continuous operation and
46 negligible loss in activity. We briefly discuss the economic trade-off of replacing the
47 traditional Pt cathode with a NPG catalyst while emphasizing the promise of NPG
48 materials to supersede precious metal catalysts in commercial PEM electrolyzers.

49
50 Recent technoeconomic analyses suggest that PEM electrolysis is a promising technology
51 for widespread renewable hydrogen production, hinging on capital cost reductions that
52 would make this technology competitive in the hydrogen market (1). Overcoming this
53 challenge requires cost reductions across many system components, demanding
54 substantial innovation in material design, engineering, and manufacturing. Reducing
55 precious metal content has been a major R&D effort among manufacturers of PEM
56 electrolyzers, as doing so would reduce capital costs while also mitigating issues of
57 material scarcity. While Pt and Ir catalysts constitute ~8% of the total stack cost today,
58 price inelasticity, and therefore volatility, of these precious metals hinder future TW-
59 scale deployment of PEM electrolysis (2). This motivates the development of active and
60 stable NPG hydrogen evolution reaction (HER) catalysts, the best-case scenario for
61 reducing Pt content in PEM electrolyzers.

62 Inspired by hydrogen-producing enzymes such as nitrogenase, molybdenum disulphide
63 (MoS_2) emerged as one of the first promising NPG HER catalysts (3, 4). Subsequently,
64 researchers pursued similar classes of materials, including transition metal phosphides,
65 which exhibit favourable activities and stabilities in lab scale demonstrations (5–7).
66 Significant advances in the activities of NPG catalysts have been accomplished by tuning
67 the morphology, chemical composition, and crystal structure via synthesis methods (5,
68 6). Universal to nearly all published NPG HER literature are the electrochemical testing
69 protocols used to measure catalyst activity and stability (linear sweep voltammetry,
70 cyclic voltammetry, chronoamperometry, and/or chronopotentiometry) (8). Such
71 methodologies provide figures of merits such as onset potential, exchange current
72 densities, and Tafel slopes which enable benchmarking, as well as provide insightful
73 fundamental knowledge. However, relatively few studies have translated NPG catalysts
74 to PEM electrolyser devices (9–12) and to the best of our knowledge, there are no reports
75 demonstrating their integration in commercial-scale systems at relevant sizes, current
76 densities, pressures, and temperatures.

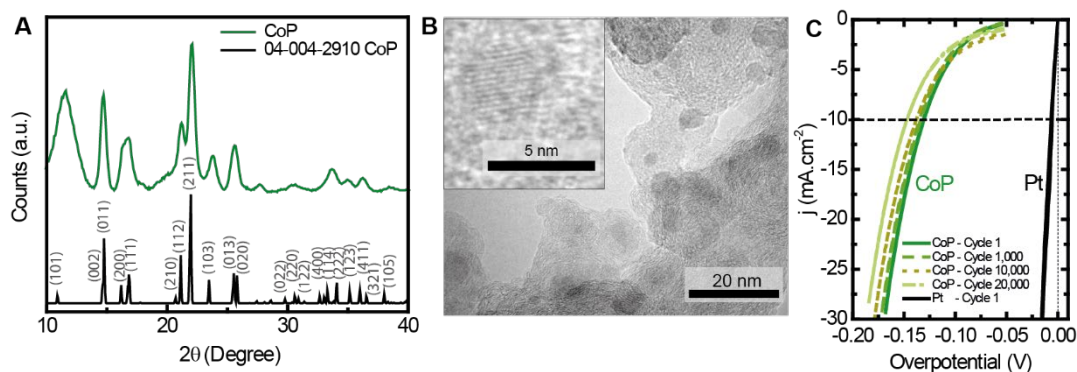
77

78 Herein, we report the first translation of a NPG HER catalyst into a commercial-scale PEM
79 electrolyser. Thanks to the development efforts of many, there were a multitude of
80 potential NPG catalyst candidates (5, 13, 14). For this first demonstration we selected
81 CoP, as experimental and theoretical studies have shown it to have promising HER
82 activity in the acidic environments relevant for PEM electrolysers (15–19). The CoP was
83 prepared by wetness impregnation of cobalt nitrate onto Vulcan carbon followed by
84 vapour phase phosphidation. The phosphidation step was adapted from a previous
85 report wherein a CoP thin film was fabricated on a silicon substrate (18). The direct
86 growth of the phosphide on the carbon support facilitates mechanical adhesion of the
87 catalyst to the substrate and enhances uniform electrical conductivity and dispersion of
88 the catalyst (6). Our simple 2-step synthesis produced >1.1 gram powder catalyst batch
89 sizes, amenable to MEA fabrication using ink-based methods. This method has the
90 potential for orders of magnitude scale-up, as batch size was only limited by the reactor
91 size employed. Synthetic details are provided in the supplementary information.

92

93 Shown in Fig. 1A is the X-ray diffraction (XRD) pattern of the as-synthesised catalyst,
94 confirming that our developed method generates a phase-pure catalyst (FeAs-type CoP).

95 X-ray photoelectron spectroscopy (XPS) of the as-prepared catalyst shows the presence
 96 of CoP, cobalt oxide, and phosphate species (Fig. S1), which are commonly reported for
 97 CoP (20). The loading of CoP on the Vulcan carbon support was $\sim 21\text{wt}\%$ with a Co:P
 98 molar ratio of 1:1, determined using inductively coupled plasma mass spectrometry (ICP-
 99 MS) (Tables S1 and S2).



100

101 **Fig. 1. Physical and electrochemical characterisation of the CoP catalyst.** (A)
 102 Powder XRD. (B) TEM micrograph. Inset shows a higher magnification micrograph of a
 103 CoP nanoparticle. (C) Linear sweep voltammograms (LSVs) (iR -corrected) of the CoP
 104 catalyst ($0.12 \text{ mg}_{\text{CoP}}.\text{cm}^{-2}$) and commercial Pt catalyst ($0.12 \text{ mg}_{\text{Pt}}.\text{cm}^{-2}$) drop cast onto
 105 carbon paper and tested in a 3-electrode electrochemical cell in $0.5 \text{ M H}_2\text{SO}_4$. LSVs are
 106 shown for the as-prepared CoP and commercial Pt (cycle 1), as well as after 1,000,
 107 10,000 and 20,000 cycles of accelerated cyclic voltammograms for the CoP catalyst.

108

109 The morphology of the catalyst was examined with transmission electron microscopy
 110 (TEM) and scanning electron microscopy (SEM) (Fig. 1B and Fig. S2). TEM enables clear
 111 identification of CoP nanoparticles with an average diameter of $\sim 5 \text{ nm}$ (Fig. 1B). HR-TEM
 112 (Fig. 1B inset) confirms lattice plane spacing of 2.5 \AA which matches FeAs-type CoP (111)
 113 (16). Lower magnification TEM micrographs show that CoP is well-dispersed on the
 114 Vulcan carbon support (Fig. S3). Thus, we report a facile synthesis route, consisting of
 115 simple precursors and few processing steps, which yields a high surface area
 116 nanoparticulate CoP catalyst that is amenable to scaled-up MEA fabrication requiring
 117 minimal technical changes.

118 Lab-scale measurements, in acidic electrolyte (Fig. 1C) revealed excellent activity and
 119 stability of the CoP catalyst (Fig. S4 and Fig. S5), in-line with previous studies (21, 22).
 120 For comparison, the activity of a commercial Pt catalyst of similar loading is also shown
 121 (Fig. 1C). While the activity of the CoP catalyst does not rival that of Pt, CoP showed little

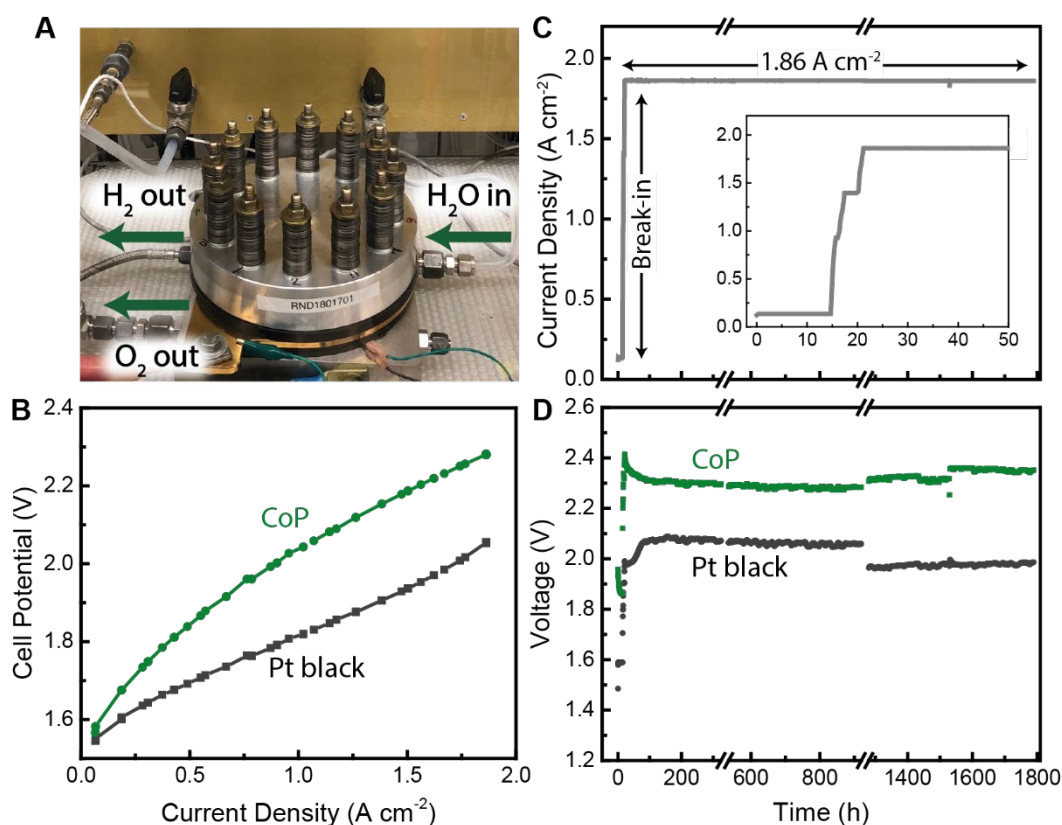
122 degradation under lab-scale cyclic voltammetry durability testing conditions and
123 reasonable onset potentials. It is well known that 3-electrode stability measurements do
124 not necessarily translate into MEA stability (23–25), which motivated further
125 examination of the CoP catalyst in a MEA. Although CoP is not the most active catalyst in
126 the literature (5), it represents a platform for performing these initial and important
127 feasibility screenings of NPG catalysts within a commercial-grade electrolyser,
128 motivating exploration of other NPG catalysts within these systems.

129 To fabricate cathode gas diffusion electrodes (GDEs), the catalyst was dispersed in a
130 suspension of Nafion ionomer, IPA, and water, then spray coated onto carbon paper gas
131 diffusion layers. The anode GDE used IrO_x as the baseline material, a known durable
132 catalyst, which isolated any observed performance changes in the electrolyser to the NPG
133 cathode. A Nafion 117 proton exchange membrane was used in the MEA, placed between
134 the anode and cathode GDEs. The MEAs were assembled in Proton OnSite's commercial
135 86 cm² active area PEM-electrolyser cell stack (Fig. 2A) along with a baseline all-PGM cell
136 (Pt black-based GDE) for direct comparison under identical operating conditions. All
137 tests were conducted at 400 psi hydrogen differential pressure and at elevated
138 temperatures with liquid water fed to the anode side of the cell. Table S3 highlights the
139 distinct differences between the 3-electrode lab-scale setup and the commercial-grade
140 testing protocol.

141 The CoP catalyst was loaded at 1.0 mg_{CoP}.cm⁻² on the GDE, equivalent to 4.5 mg.cm⁻² total
142 catalyst loading including the carbon support. The electrolyser was first characterised
143 by stepping the current from 100 mA.cm⁻² (1.54V) to 1.86 A.cm⁻² (2.27 V) at 50 °C (Fig.
144 2B). Interestingly, the polarisation curve shows this non-precious catalyst can reach the
145 same high current densities as the Pt-containing cell at reasonable potentials. Assuming
146 that every unit of CoP is active for the HER, a conservative estimate for the turnover
147 frequency (TOF) of CoP is 0.87 H₂.s⁻¹. More likely, only the surface bound CoP units (~10
148 %) participate in the reaction, leading to an estimated TOF_{avg} of 8.7 H₂.s⁻¹. Comparatively,
149 the TOF for the Pt catalyst is estimated to be 1.88 H₂.s⁻¹ conservatively, or 28.8 H₂.s⁻¹
150 assuming only surface atoms participate in the reaction. Details of the calculations are
151 shown in the supplementary information.

152 The all-PGM baseline GDE shows that the Pt PEM required 2.05 V to reach a current
153 density of 1.86 A.cm⁻² (Fig. 2B). This result reflects operating efficiencies of 55% and 61%

154 respectively for the CoP- and Pt-based electrolyzers based on the lower heating value
 155 (LHV). While the fact that the Pt system performs 220 mV better than the NPG catalyst is
 156 not surprising given the 3-electrode measurements (Fig. 1C), this small difference is
 157 impressive considering the commercially relevant high current densities employed.
 158 Future work will explore electrode engineering to maximize the performance of NPG
 159 based electrolyzers. Optimization of catalyst loading and ionomer content, for example,
 160 will only help to narrow the performance gap between PGM and NPG catalysts in
 161 commercial electrolyser platforms. This gap will continue to shrink as NPG catalysts
 162 themselves are further improved, minimizing the trade-offs between operating and
 163 capital costs (14).



164

165 **Fig. 2. PEM electrolyser performance.** (A) Photograph of the 86 cm² electrolyser test
 166 station. (B) Polarisation curve. (C) Current density profile for the durability protocol.
 167 The inset shows the current density profile for the break-in period only. (D) Durability
 168 voltage-time plots for the PEM electrolyser prepared with 1.0 mg_{CoP}.cm⁻² loading while
 169 operating at 50 °C and 400 psi. Voltage discontinuities result from power outage-induced
 170 restarts.

171

172 The CoP and Pt-based MEA durability tests were also conducted in the 2-cell stack
173 following the polarisation studies. The differences in operating conditions between the
174 2-electrode and 3-electrode stability measurements are noted in Table S3. The tests were
175 initiated at 50 °C and held at 0.135 A.cm⁻² for ~20 h (Fig. 2C and 2D). After 20 h of
176 operation, the temperature was ramped to 55 °C and the current was increased to 1.86
177 A.cm⁻² over 6 h. The current density was subsequently held at 1.86 A.cm⁻² for the
178 remaining 1763 h of testing. During the durability measurement, the CoP MEA stabilised
179 within 50 h to provide steady operation at 2.30 V for >900 h with energy consumption of
180 60.4 kWh.kg_{H2}⁻¹. The Pt-based MEA operated under the same conditions (1.86 A.cm⁻², 55
181 °C, 400 psi) at 2.06 V as expected without degradation, corresponding to energy
182 consumption of 54.5 kWh.kg_{H2}⁻¹. Transient behaviour in the break-in phase is discussed
183 in the supplementary information.

184 After 922 h of continuous testing, the 2-cell stack (CoP and Pt MEAs) lost power briefly
185 (<1 min) and was restarted. The reset resulted in an increase (~50 mV) in cell potential
186 for the CoP MEA and a slightly reduced potential for the Pt MEA (~6 mV). A second, small
187 abrupt increase in potential was observed after 1550 h of operation, likely due to a second
188 disruption in the applied potential. Duplicate CoP and Pt MEAs were fabricated and
189 tested with a similar protocol and were shown to be extremely stable with comparable
190 cell potentials (Fig. S6). Discussion of the MEA restarts and characterisation of the CoP
191 GDE after the 1700 h durability test are provided in the supplementary information (Fig.
192 S7). Analogous to the fuel cell literature, it is important to note that Pt-based commercial
193 PEM electrolyzers are also known to degrade on start-up and shut-down cycling and
194 hence this challenge is relevant for all known catalysts, precious metal and non-PGMs
195 alike (26).

196 In a 3-electrode lab-scale configuration, it has been reported that non-precious metal
197 ionic compound catalysts such as transition metal phosphides dissolve at higher rates
198 under OCP conditions, but are stable when evolving hydrogen, even when cycling from
199 low to high production rates (27, 28). This report is consistent with our lab-scale
200 durability measurements of CoP dissolution during electrochemical testing (Fig. S8 and
201 Fig. S9). We therefore postulate that CoP dissolution occurred when the MEA lost power
202 briefly after 922 h and 1550 h of operation leading to the increased cell potential.

203 Furthermore, we propose operating procedures that maintain a small operating current
204 could prevent this degradation mechanism.

205 Remarkably, the CoP MEA produced a total of 10.1 kg of H₂ (912 L at STP), and we
206 conservatively estimate a turnover number (TON) of 5.3 x 10⁶ H₂ molecules produced per
207 CoP site assuming all CoP units are active. Details of the calculations are shown in the
208 supplementary information. The CoP MEA requires 12 – 18 % greater power density
209 than the Pt baseline MEA, a potentially attractive trade-off between electricity
210 consumption and electrolyser capital cost depending on the application and the local cost
211 of electricity. While this work highlights a significant step towards non-PGM catalyst
212 incorporation in commercial electrolysers, the difference in performance between CoP
213 and Pt is still too substantial for wide-scale commercial deployment, motivating
214 continued research and development of non-PGM catalysts.

215 Analyses show that the levelized cost of hydrogen (LCH) from water electrolysis is
216 currently dominated by the cost of electricity (29, 30). However, as society follows a path
217 towards increased electrification and electricity prices drop, the capital cost of
218 electrolysers will begin to dominate (31, 32). Utilisation of durable, low-cost NPG
219 catalysts that can replace expensive and price inelastic precious metals is one critical step
220 towards reducing the overall capital cost of PEM electrolysis (Table S4). While the result
221 presented here is a significant achievement, we note that cost reductions across all
222 system components are needed for TW-scale deployment of PEM electrolysers. A full
223 techno-economic analysis on the implications of this report is outside the scope and will
224 be the subject of future investigations.

225 Our initial demonstration of an active and highly stable NPG HER catalyst in a
226 commercial-scale PEM electrolyser highlights the practical relevance of NPG systems. By
227 extending our lab-scale stability study from liquid electrolyte and 1 cm² electrode area to
228 an 86 cm² commercial PEM electrolyser with >1700 h of stable operation at elevated
229 temperature and pressure, we demonstrate the commercial relevance of NPG catalysts.
230 Compared to a Pt-based PEM, we found the CoP PEM to pay a 12 – 18 % power penalty
231 under the operating conditions, but to provide a significant improvement in material cost
232 over the commercial Pt catalyst. We believe that the results represent a possible entry
233 point for NPG catalyst utilisation in commercial water electrolysers. Continued research
234 efforts between industry and academia enables pathways to lowering the capital

235 investment costs of PEM electrolyzers while maintaining high operating efficiencies to
236 implement grid-scale energy storage.

237 **Methods**

238 Methods, including statements of data availability are available in the Supplementary
239 Information.

240

241 **References and Notes**

- 242 1. L. Bertuccioli *et al.*, Study on development of water electrolysis in the EU. *Fuel Cells*
243 *Hydrog. Jt. Undert.*, 1–160 (2014).
- 244 2. P. C. K. Vesborg, T. F. Jaramillo, Addressing the terawatt challenge: scalability in the
245 supply of chemical elements for renewable energy. *RSC Adv.* **2**, 7933 (2012).
- 246 3. B. Hinnemann *et al.*, Biomimetic Hydrogen Evolution: MoS₂ Nanoparticles as Catalyst for
247 Hydrogen Evolution. *J Am Chem Soc.* **36**, 5308–5309 (2005).
- 248 4. T. F. Jaramillo *et al.*, Identification of Active Edge Sites for Electrochemical H₂ Evolution
249 from MoS₂ Nanocatalysts. *Science (80-)*. **317**, 100–102 (2007).
- 250 5. J. F. Callejas, C. G. Read, C. W. Roske, N. S. Lewis, R. E. Schaak, Synthesis , Characterization ,
251 and Properties of Metal Phosphide Catalysts for the Hydrogen-Evolution Reaction. *Chem.*
252 *Mater.* (2016), doi:10.1021/acs.chemmater.6b02148.
- 253 6. Y. Shi, B. Zhang, Recent advances in transition metal phosphide nanomaterials: synthesis
254 and applications in hydrogen evolution reaction. *Chem. Soc. Rev.* **45**, 1529–1541 (2016).
- 255 7. J. Kibsgaard, T. F. Jaramillo, Molybdenum phosphosulfide: An active, acid-stable, earth-
256 Abundant catalyst for the hydrogen evolution reaction. *Angew. Chemie - Int. Ed.* **53**,
257 14433–14437 (2014).
- 258 8. C. C. L. McCrory *et al.*, Benchmarking Hydrogen Evolving Reaction and Oxygen Evolving
259 Reaction Electrocatalysts for Solar Water Splitting Devices. *J. Am. Chem. Soc.* **137**, 4347–
260 4357 (2015).
- 261 9. T. Corrales-Sánchez, J. Ampurdanés, A. Urakawa, MoS₂-based materials as alternative
262 cathode catalyst for PEM electrolysis. *Int. J. Hydrogen Energy.* **39**, 20837–20843 (2014).
- 263 10. J. W. D. Ng *et al.*, Polymer Electrolyte Membrane Electrolyzers Utilizing Non-precious Mo-
264 based Hydrogen Evolution Catalysts. *ChemSusChem.* **8**, 3512–3519 (2015).
- 265 11. C. Di Giovanni *et al.*, Low-Cost Nanostructured Iron Sulfide Electrocatalysts for PEM
266 Water Electrolysis. *ACS Catal.* **6**, 2626–2631 (2016).
- 267 12. X. Sun *et al.*, Earth-Abundant Electrocatalysts in Proton Exchange Membrane
268 Electrolyzers. *Catalysts.* **8**, 657 (2018).
- 269 13. S. Anantharaj *et al.*, Recent Trends and Perspectives in Electrochemical Water Splitting
270 with an Emphasis on Sulfide, Selenide, and Phosphide Catalysts of Fe, Co, and Ni: A
271 Review. *ACS Catal.* **6**, 8069–8097 (2016).
- 272 14. P. Xiao, W. Chen, X. Wang, A Review of Phosphide-Based Materials for Electrocatalytic

- 273 Hydrogen Evolution. *Adv. Energy Mater.* **5**, 1–13 (2015).
- 274 15. W. Liu *et al.*, A highly active and stable hydrogen evolution catalyst based on pyrite-
275 structured cobalt phosphosulfide. *Nat. Commun.* **7**, 1–9 (2016).
- 276 16. E. J. Popczun, C. G. Read, C. W. Roske, N. S. Lewis, R. E. Schaak, Highly Active
277 Electrocatalysis of the Hydrogen Evolution Reaction by Cobalt Phosphide Nanoparticles
278 ** *Angewandte. Angew. Chemie - Int. Ed.*, 5531–5534 (2014).
- 279 17. J. Kibsgaard *et al.*, Designing an improved transition metal phosphide catalyst for
280 hydrogen evolution using experimental and theoretical trends. *Energy Environ. Sci.* **8**,
281 3022–3029 (2015).
- 282 18. T. R. Hellstern, J. D. Benck, J. Kibsgaard, C. Hahn, T. F. Jaramillo, Engineering Cobalt
283 Phosphide (CoP) Thin Film Catalysts for Enhanced Hydrogen Evolution Activity on
284 Silicon Photocathodes. *Adv. Energy Mater.* (2016), doi:10.1002/aenm.201501758.
- 285 19. Z. Wu, L. Huang, H. Liu, H. Wang, Element-Specific Restructuring of Anion- and Cation-
286 Substituted Cobalt Phosphide Nanoparticles under Electrochemical Water-Splitting
287 Conditions. *ACS Catal.* **9**, 2956–2961 (2019).
- 288 20. F. H. Saadi *et al.*, Operando Spectroscopic Analysis of CoP Films Electrocatalyzing the
289 Hydrogen-Evolution Reaction. *J. Am. Chem. Soc.* **139**, 12927–12930 (2017).
- 290 21. H. Yang, Y. Zhang, F. Hu, Q. Wang, Urchin-like CoP Nanocrystals as Hydrogen Evolution
291 Reaction and Oxygen Reduction Reaction Dual-Electrocatalyst with Superior Stability.
292 *Nano Lett.* **15**, 7616–7620 (2015).
- 293 22. D. Zhou *et al.*, Interconnected urchin-like cobalt phosphide microspheres film for highly
294 efficient electrochemical hydrogen evolution in both acidic and basic media. *J. Mater.*
295 *Chem. A*, **4**, 10114–10117 (2016).
- 296 23. S. Martens *et al.*, A comparison of rotating disc electrode, floating electrode technique and
297 membrane electrode assembly measurements for catalyst testing. *J. Power Sources.* **392**,
298 274–284 (2018).
- 299 24. S. M. Alia *et al.*, Activity and Durability of Iridium Nanoparticles in the Oxygen Evolution
300 Reaction. *J. Electrochem. Soc.* **163**, F3105–F3112 (2016).
- 301 25. S. M. Alia, B. S. Pivovar, Iridium-Based Nanowires as Highly Active, Oxygen Evolution
302 Reaction Electrocatalysts. *ACS Catal.* **8**, 2111–2120 (2018).
- 303 26. A. Weiß, A. Siebel, M. Bernt, H. A. Gasteiger, Impact of Intermittent Operation on the
304 Lifetime and Performance of a PEM Water Electrolyzer. *Meet. Abstr.* . **MA2018-02**, 1606
305 (2018).
- 306 27. Y. Zhang, L. Gao, E. J. M. Hensen, J. P. Hofmann, Evaluating the Stability of Co₂P
307 Electrocatalysts in the Hydrogen Evolution Reaction for Both Acidic and Alkaline
308 Electrolytes. *ACS Energy Lett.*, 1360–1365 (2018).
- 309 28. M. Ledendecker *et al.*, Stability and Activity of Non-Noble-Metal-Based Catalysts Toward
310 the Hydrogen Evolution Reaction. *Angew. Chemie.* **129**, 9899–9903 (2017).
- 311 29. B. James, W. Colella, J. Moton, G. Saur, T. Ramsden, PEM Electrolysis H₂A Production Case
312 Study Documentation. *PEM Electrolysis H₂A Prod. Case Study Doc.*, 1–27 (2013).
- 313 30. U. Babic, M. Suermann, F. N. Büchi, L. Gubler, T. J. Schmidt, Critical Review—Identifying
314 Critical Gaps for Polymer Electrolyte Water Electrolysis Development. *J. Electrochem. Soc.*
315 **164**, F387–F399 (2017).

316 31. I. Introduction, Introduction - DOE 2013 Hydrogen and Fuel Cells Program Annual
317 Progress Report (2017).

318 32. F. Cell, T. Office, N. Renewable, 2017 H2 @ Scale Workshop Report (2017).

319

320 **Acknowledgements:**

321 Physical characterisation of the catalyst in this work was performed at the Stanford Nano
322 Shared Facilities (SNSF), supported by the National Science Foundation under award
323 ECCS-1542152. We thank Richard Chin for his assistance with scanning electron
324 microscopy at this facility.

325

326 **Funding:** We acknowledge DoD SBIR Phase I Contract Number: N00024-17-P-4507,
327 topic Number: N162-107 for financial support and the project manager Joshua Manney.
328 The US Department of Energy (DOE) Office of Basic Energy Sciences (BES) is
329 gratefully acknowledged for support for the SUNCAT Center for Interface Science and
330 Catalysis for fundamental catalysis development. M.A.H acknowledges the support of a
331 National Science Foundation Graduate Research Fellowship.

332

333 **Authors contributions:** L.A.K. and M.A.H. contributed equally to this work. L.A.K., M.A.H.,
334 and T.R.H. synthesized CoP catalysts. L.A.K. performed x-ray diffraction and scanning
335 electron microscopy characterisation. E.V. performed transmission electron microscopy
336 characterisation. M.A.H. performed electrochemical lab-scale characterisation and
337 testing. C.C., J.M., and N.D. prepared all PEM stack components, assembled and tested the
338 electrolyser, as well as collected all operational data. L.A.K. and M.A.H. contributed to
339 data analysis, including preparation and revision of this manuscript.

340

341 **Competing interests:** None.

342

343 **Data and materials availability:** The x-ray diffraction reference pattern is available
344 from the Materials Project database under the ID mp-22270. Full synthetic details,
345 electrochemical testing protocols, and raw data can be found in the supplementary
346 information section.

347

348	Supplementary Information
349	Materials and Methods
350	Figures S1 – S9
351	Table S1 – S4
352	Turnover frequency and turnover number estimations
353	Electrolyser efficiency calculations
354	